Available online at www.sciencedirect.com
ScienceDirect
International Journal of Thermal Sciences 47 (2008) 1454–1463
International Journal of Thermal Sciences
www.elsevier.com/locate/ijts

Characterization of Marangoni effect in non-isothermal falling liquid films of binary mixtures

Feng Zhang [a,b], Xian-Guang Zhao [b], You-Ting Wu [b], Zhi-Xiang Wang [a], Zhi-Bing Zhang [b,*]

[a] *Department of Pharmaceutical Engineering, China Pharmaceutical University, Nanjing 210009, China*
[b] *School of Chemistry and Chemical Engineering, Nanjing University, Nanjing 210093, China*

Received 1 March 2007; received in revised form 30 July 2007; accepted 5 October 2007

Available online 30 January 2008

Abstract

The flow characteristics and heat transfer were investigated for the liquid films of water, ethanol aqueous solution, glycerol aqueous solution and aqueous Na_2SO_4 solution. By using a sensitive thermal imaging system, the temperature and liquid distributions of the film could be carefully studied to reveal the influence of Marangoni effect on the heat transfer and flow of the binary mixture films. Since the surface tension gradient and surface tension counteracted on the film, a surface tension factor was presented to describe the surface tension effect in the films and help designing the experiments. It was concluded to be the thermal Marangoni effect that caused the cooled films expanded and the heated films contracted. A novel expansion was found for the heated ethanol aqueous film, due to the concentration variation and so-caused solutal Marangoni flow that overcame the thermal Marangoni flow in the lateral direction of the film. Theoretical analysis also indicated that the solutal Marangoni effect was more effective than the thermal Marangoni effect. Furthermore, viscosity has a complex influence on the Marangoni flow. Larger viscosity generally caused greater temperature gradient, and thus enhanced surface tension gradient (Marangoni flow), meanwhile, all the liquid flow (including Marangoni flow) were retarded due to the more significant viscous resistance.

Keywords: Falling liquid films; Heat transfer; Surface tension gradient; Temperature variations; Marangoni effect

1. Introduction

Falling liquid films are widely employed in the heat and mass transfer processes of the industrial equipments, including vertical condensers, film evaporators, absorption towers and seawater desalinators. The phenomena in the falling film, such as formation of surface waves, breaking of a stream into rivulets, evaporation at a contact line, and liquid maldistribution, are frequently encountered and have significant influence on the transfer processes. Thereby, the good understanding of these phenomena helps to improve the predictions of heat and mass transfer rates in the film devices.

In recent years, the flow characteristics, transfer processes and the interfacial instabilities, especially the Marangoni effect in the non-isothermal film have been widely investigated by using theoretical and experimental methods. The Marangoni flow, which is fluid flow induced by surface tension gradient (due to the variations of concentration or temperature), proceeds from regions of lower surface tension to those of higher surface tension. In 1959, Scriven and Sternling made the linear stability analysis for the solute Marangoni flow [1]. The next year, they [2] reviewed the study of the Marangoni effect. Cazabat et al. [3] also performed excellent work to study the fingering instability of thin spreading films that were driven by temperature gradient. They revealed that lower viscosity and greater temperature gradient reinforced the Marangoni flow. Recently, Aubeterre [4] experimentally investigated the Marangoni effect induced by heat and mass transfer of four aliphatic alcohol (from C1 to C4), exploring that Marangoni number decreased with the increasing carbon number atoms (n), due to the changes of some physical properties (surface tension, diffusivity, viscosity) as heat and mass transfer occurred.

It was reported that the Marangoni effect induced by the temperature gradient or concentration variations was desta-

* Corresponding author.
E-mail address: segz@nju.edu.cn (Z.-B. Zhang).

1290-0729/$ – see front matter
doi:10.1016/j.ijthermalsci.2007.10.021

Nomenclature

Roman

A	interfacial area of falling film	m^2
B	positive constant	
c	mass fraction	
$C_{Na_2SO_4}$	mass fraction of Na_2SO_4	
C_p	specific heat at constant pressure	$kJ\,kg^{-1}\,K^{-1}$
E	mass fraction of ethanol	
F	parameter	
g	the gravity acceleration	
G	mass fraction of glycerol	
h	heat transfer coefficient	$W\,m^{-2}\,K^{-1}$
F	parameter	
L	length of heating region	m
Ma	Marangoni number	
Nu	Nusselt number	
Q	volume flow rate	$m^3\,s^{-1}$
Re	Reynolds number	
S	surface tension factor	
V	molar volume	

Greek symbols

a	thermal diffusivity	$m^2\,s^{-1}$
ϕ	volume fraction	
θ	contact angle	
γ	surface tension coefficient	
μ	dynamic viscosity	Pa s
ν	kinematics viscosity	$m^2\,s^{-1}$
ρ	density of liquid	$kg\,m^{-3}$
σ	surface tension	$N\,m^{-1}$
λ	liquid thermal conductivity	$W\,m^{-1}\,K^{-1}$
Γ	mass flow rate	$kg\,m\,s^{-1}$

Subscripts

0	initial
A	water
B	organic compound
c	critical
f	average film temperature
T	temperature
h	heat
m	mixture
out	outlet of falling film
s	surface of liquid film
soln	solution
w	wall

bilizing whereas capillarity and evaporation were stabilizing processes [5–7]. Kabov Group [8] discovered that the instabilities of a thin locally heated falling film, which was caused by the Marangoni effect, probably resulted in a decrease of the heat transfer coefficient with the increasing Reynolds number. Joo [9,10] discovered that the thermo-capillary instability was dominant due to the absence of gravity-driven flow in the lateral direction, inducing the spontaneous film rupture. Zhang [11,12] also investigated the heated water films, revealing that the heated water films were evidently contracted in the lateral direction by the transverse surface tension gradient. This is quite similar to the non-isothermal spreading of liquid drops on heated (cooled) horizontal plates. For these drops, Ehrhard and Davis [13] proved that heating (cooling) retarded (augmented) the spreading process by creating surface tension gradient driven flows.

Some researchers [14–16] paid special attentions to the heat and mass transfer enhancement of the LiBr aqueous film by Marangoni effect resulted from adding surfactants into the film. Sun [17] successfully obtained the expressions for the liquid-phase mass and heat transfer rate enhanced by Rayleigh–Benard–Marangoni cellular convection. Furthermore, Hosoi and Bush [7] discovered that the evaporation of ethanol– or methanol–water solution led to concentration variations, causing the surface tension gradients that drove flow up an inclined rigid plate. It was also found that the condensation heat transfer of binary mixture vapor was enhanced by Marangoni effect which produced a disturbed, turbulent banded condensate film [18,19].

The films of binary solutions are more frequently used in the industry and should be further investigated to optimize the operation and designing of the falling film equipments. The thermal imaging research on the falling liquid films is very useful to make clear the inducement and behavior of Marangoni effect. In the present work, the heated/cooled films of water, ethanol aqueous solution (volatile liquid), glycerol aqueous solution (viscous liquid) and aqueous Na_2SO_4 solution (electrolyte aqueous liquid) were investigated. Based on the theoretical analyses of surface tension effect, the experiments were carefully designed. The experimental data allowed analyzing the influences of film flow rate, viscosity, surface tension, liquid concentration and heating conditions on the heat transfer, surface temperature gradient and liquid distributions of the heated/cooled film. Thus the influence of Marangoni effect on the heat transfer and flow of the binary mixture films could be determined. Moreover, the contributions of temperature and concentration variations to the surface tension gradient were compared.

2. Experimental apparatus

The experiment scheme is illustrated in Fig. 1. In each run of the experiment, the liquid in the reservoir was maintained a preset temperature and was pumped to the upper tank. Then it flowed through a rotameter to the liquid distributor, in which the liquid film about 8.5 cm wide was formed. The liquid film then flowed down over the test section (a vertical smooth stainless steel plate about 600 mm wide and 400 mm long) whose backside was heated with water at a scheduled temperature T_h, and

was finally collected and sent back to the liquid reservoir. In the experiments, the film temperatures T_0 and T_{out}, the temperature of the ambient air and the heating temperature T_h were all measured with Pt-100 thermal resistances under an uncertainty of $\pm 0.1\,^{\circ}C$. The most important part of the experimental apparatus was Thermal Imaging System (manufactured by Flir System Company, USA) with which the temperature field and shape of the film could be recorded and analyzed by professional software. The accuracy of this thermal camera is $\pm 0.1\,^{\circ}C$. The distance between the film and the thermal camera is 0.60 m, and at that distance, the spacing resolution of the camera is 0.6 mm. In the experiments, a ruler is located on the plate to obtain the ratio of real dimension and dimension measured from the thermal image, therefore the surface temperature gradient and the width of the film could be calculated from the coordinates of the film in the thermal images (the average deviation of the film width was less than 2%). Then the film interfacial area was calculated with the values of the film widths and the distances down from the upper edge of the heater. Duplicate experiments for each run were performed to obtain the average values of film width at different location and the interfacial area.

Distilled water, ethanol aqueous solutions (0.05–0.1), glycerol aqueous solutions (0.05–0.5) and Na_2SO_4 aqueous solutions (0.01–0.1) were used to investigate the influence of viscosity and surface tension gradients on the heat transfer and liquid distribution of the films. In particular, the effects of operating conditions such as liquid flow rate and heating condition were also evaluated. For weakening the influence of evaporation, the test section was placed in a closed transparent shell. In each run of experiment, the concentrations of solutions were monitored by the Anton Paar DMA5000 Density-Meter to make sure that the concentration did not vary too much, otherwise, a quantitative solute would be added to keep the concentration. All the measurements were done after the system had stabilized for a given condition. The physical characteristics of working fluids and the basic experiment parameters are given in Table 1.

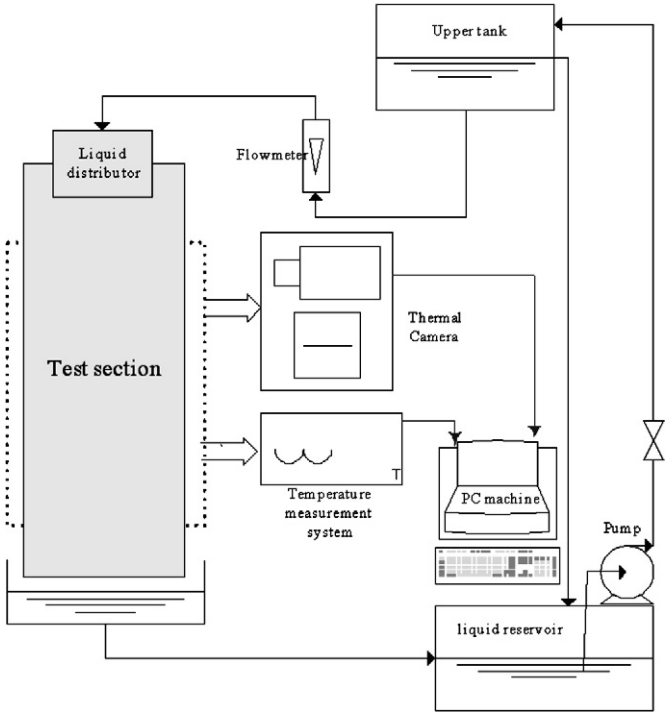

Fig. 1. Sketch diagram of the experimental system.

3. Results

3.1. Surface tension factor

In the liquid films, the effects of surface tension gradient and surface tension are contrary, i.e., surface tension gradient is to destabilize the film, while the surface tension is to stabilize the film [20]. Thus it is necessary to use the factor S to characterize the surface tension effect (including the effects of surface tension and its gradient) in the film flow [3]. Practically, surface tension of the binary mixture is determined by temperature and concentration of the solute. According to the factor with which the surface tension varies, S can be written in the following two formations:

$$\text{concentration variations:} \quad S_c = \frac{1}{\sigma}\frac{\mathrm{d}\sigma}{\mathrm{d}c} \tag{1}$$

$$\text{temperature variations:} \quad S_T = \frac{1}{\sigma}\frac{\mathrm{d}\sigma}{\mathrm{d}T} \tag{2}$$

where, σ, T and c are the liquid surface tension, temperature and the weight fraction of the solution.

In this work, the surface tension of glycerol aqueous solution and ethanol aqueous solution is calculated with Tumura–Kurata–Odani method. The surface tension of an organic aqueous mixture can be obtained from Eq. (3)

$$\sigma_m^{1/4} = \phi_{sA}\sigma_A^{1/4} + \phi_{sB}\sigma_B^{1/4} \tag{3}$$

where, subscripts A and B denote water and organic compound, respectively. ϕ_{sA} and ϕ_{sB} can be obtained by the following equations:

$$\phi_{sA} + \phi_{sB} = 1, \qquad C_A = C_B + F$$
$$C_A = \lg\left(\phi_{sA}^q/\phi_{sB}\right), \qquad C_B = \lg\left(\phi_A^q/\phi_B\right)$$

Table 1
Physical characteristics of working fluids and operation parameters

Physical characteristics	Operation parameters
Density ρ: 984.2–1037.2 kg/m^3	Flow rate Γ: 0.03–0.37 kg/(m s)
Viscosity μ: 7.64×10^{-4}–130.0×10^{-4} Pa s	Initial temperature T_0: 25–50 °C
Surface tension σ: 43.9–73.3 dyn/cm	Heating temperature T_h: 0–70 °C
Heat conductivity λ: 0.472–0.647 W/(m K)	Reynolds number $Re = 4\Gamma/\mu$: 42–3173
Thermal capacity C_p: 75.2–97.7 J/(mol K)	Prandtl number $Pr = C_P\mu/\lambda$: 4.79–109.5

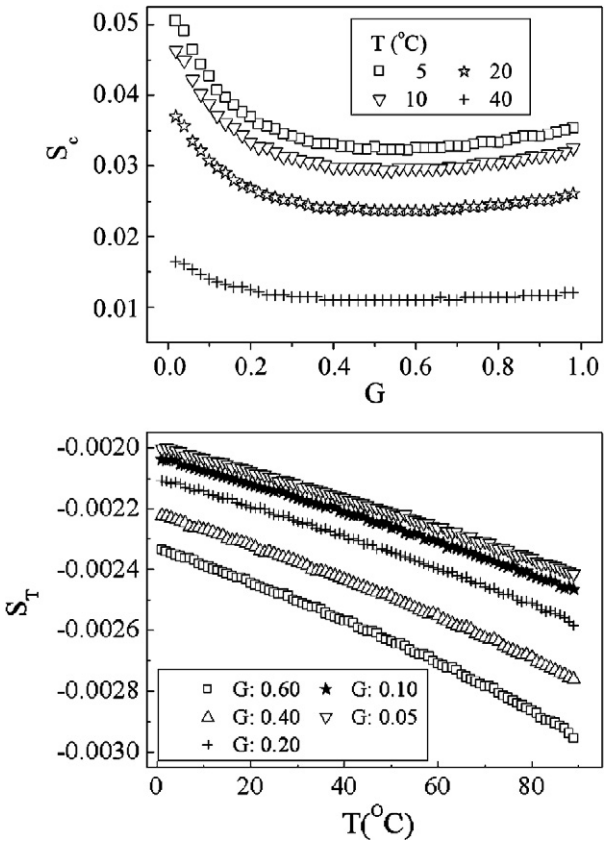

Fig. 2. S for the glycerol aqueous solutions. G: the weight fraction of glycerol.

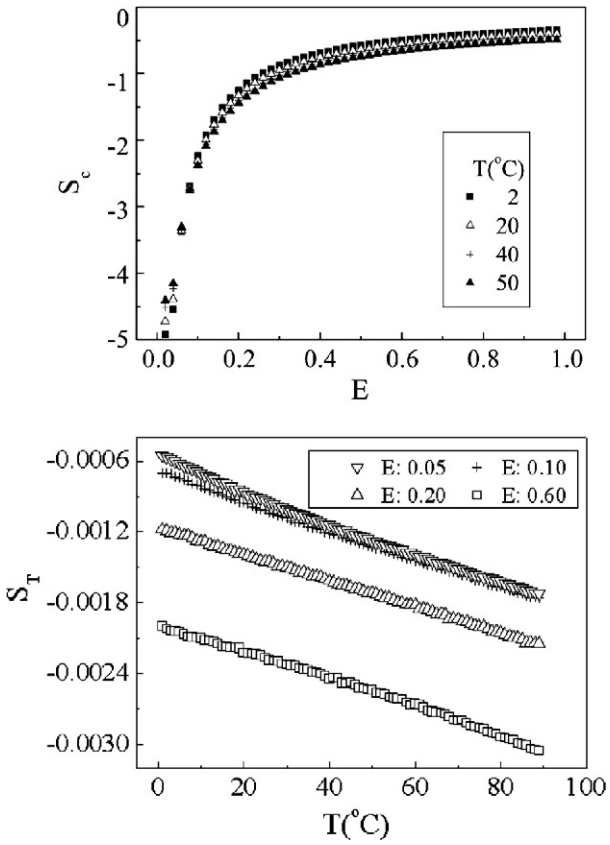

Fig. 3. S for ethanol aqueous solutions. E: the weight fraction of ethanol.

$$F = 0.441(q/T)\left(\frac{\sigma_B V_B^{2/3}}{q} - \sigma_A V_A^{2/3}\right)$$

$$\phi_A = \frac{x_A V_A}{x_A V_A + x_B V_B}, \qquad \phi_B = \frac{x_B V_B}{x_A V_A + x_B V_B} \tag{4}$$

where, the subscript s stands surface of the mixture. x_A and x_B are mole concentrations of A and B, respectively. The parameter q is determined by the size and structure of the organic compound.

For the glycerol–water mixture, as illustrated in Fig. 2, S_c is positive due to the increase of surface tension with a rise in glycerol concentration. An increase of the temperature results in reduced S_c. Under the same T, S_c drops with the increasing glycerol concentration G until $G = 0.3$, then it rises slightly with a further increase in glycerol concentration. On the other hand, S for the temperature variation, S_T is negative since surface tension decreases with the increasing temperature of the liquid. As shown in Fig. 2, the higher T leads to the less S_T of the glycerol–water mixture, and at a given temperature, increasing G results in decreasing S_T. Obviously, for the glycerol–water mixture, $|S_c|$ is one order of magnitude larger than $|S_T|$, implying that the concentration variations is able to cause greater surface tension effect than the temperature variations.

Contrary to the glycerol–water system, S_c of the ethanol–water solutions is negative, due to the decrease of surface tension with the increasing ethanol concentration. It is shown in Fig. 3 that S_c moves up sharply with a rise in ethanol concentration E when E is less than 0.3, and then it rises slightly as E further increases. Whereas, S_T drops with the increasing E. Unlike the case of glycerol–water mixture, temperature seems to have no influence on S_c for the ethanol–water mixture. It can also be found in Fig. 3 that $|S_c|$ is at least 300 times higher than $|S_T|$ for the ethanol–water mixture.

For the aqueous Na_2SO_4 solution, S can be calculated by $S_c = B/(1 + Bc)$ and $S_T = \gamma/(\sigma^o_{H_2O} + \gamma T)$, since the surface tension of the aqueous Na_2SO_4 solution can be obtained by the following correlation [21]:

$$\sigma_{\text{soln}} = \sigma_A(1 + Bc) = (1 + Bc)\left(\sigma^o_A + \gamma T\right) \tag{5}$$

where, c denotes to the weight fraction of solute. B is a positive constant and $\gamma = \partial\sigma/\partial T$ the surface tension coefficient of water. S_c and S_T for the aqueous Na_2SO_4 solution are plotted in Fig. 4, showing that the positive S_c is independent of the temperature, but decreases with the increasing Na_2SO_4 concentration. On the other hand, the higher temperature leads to larger $|S_T|$, while the concentrations seem to have no influence on S_T.

The comparisons of Fig. 2 with Figs. 3 and 4 show that S_T of these three mixtures is quite similar to each other, i.e., S_T is negative and decreases with the temperature increasing. Whereas $|S_c|$ of ethanol–water solution is significantly larger than those of aqueous Na_2SO_4 solution and glycerol–water solution, especially when the concentrations are less than 0.3. This indicates that more surface tension gradient might be induced by the concentration variations in the ethanol–water film.

As mentioned above, $|S_c|$ is much higher than $|S_T|$ for the all working liquids utilized in present work.

In general, increasing concentration results in larger $|S_T|$ for the ethanol aqueous solution and glycerol aqueous solution, implying that significant Marangoni flow may occur for the larger concentrations. However, much high concentration probably causes great viscosity for the glycerol–water mixture, and distinct evaporation of ethanol for the ethanol–water mixture, inducing many difficulties in the experimental operations. As for the aqueous Na_2SO_4 solution, decreasing concentration resulted in enhanced S_c. Therefore, in the present work, the suitable concentrations of these three solutions are selected, with E ranging from 0.05 to 0.15, G in the range of 0.10–0.50, and the concentration of Na_2SO_4 in the range of 0.01–0.10.

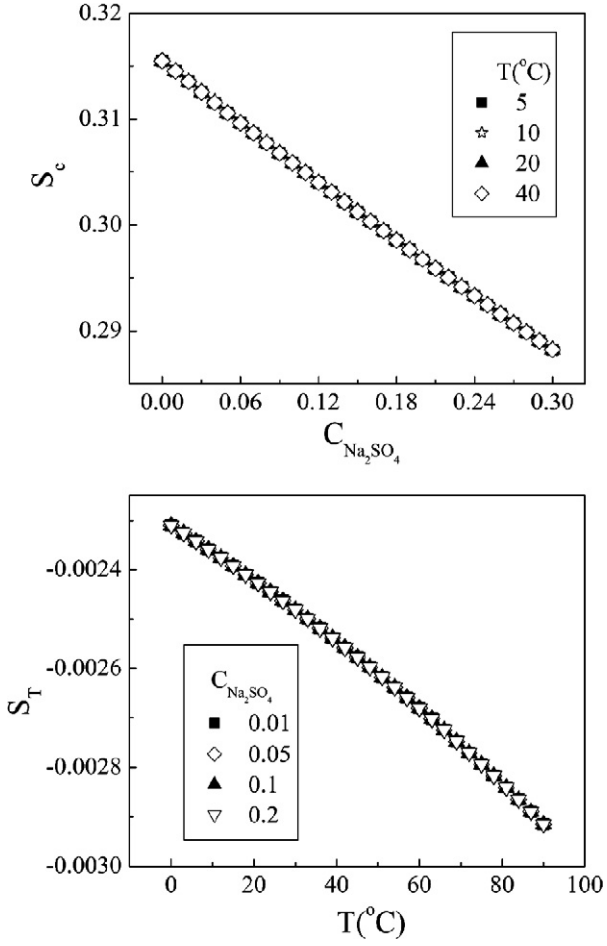

Fig. 4. S for the aqueous Na_2SO_4 solutions. $C_{Na_2SO_4}$: the weight fraction of Na_2SO_4.

3.2. Experimental results and discussion

Thermal Marangoni effect is inevitable in the liquid film flowing over a heated solid surface. For the water film, lateral surface temperature gradient generated the Marangoni effect that caused the contraction/extension of heated/cooled films [11,12]. In this work, the contraction or extension is also found in the ethanol–water films, glycerol–water films and aqueous Na_2SO_4 films. The thermal images of these films are illustrated in Fig. 5, where different colors represent different temperature magnitudes, the darker the color, the lower the temperature. For well understanding the Marangoni effect in the films, we choose Cartesian axes as indicated in Fig. 5, with x axis in the direction of flow and z axis horizontal (transverse to the direction of flow) with respect to which the substrate is denoted by $y = 0$. As can be seen, the lateral temperature variations (especially in the film rim) are greater than the streamwise temperature variations, probably causing prominent Marangoni flow in that direction. It is notable that driven by the thermal Marangoni flow (shown as arrow 1), the heated glycerol aqueous film and aqueous Na_2SO_4 film ($T_0 < T_h$) are contracted gradually to form an inverse trapezoid, whereas the cooled films ($T_0 > T_h$) are extended slightly by the thermal Marangoni flow (shown as arrow 2) to form a right trapezoid. The cooled ethanol–water film is also extended, while the heated ethanol–water film is surprisingly enlarged. This extension of the heated ethanol–water film can be explained by taking into account the

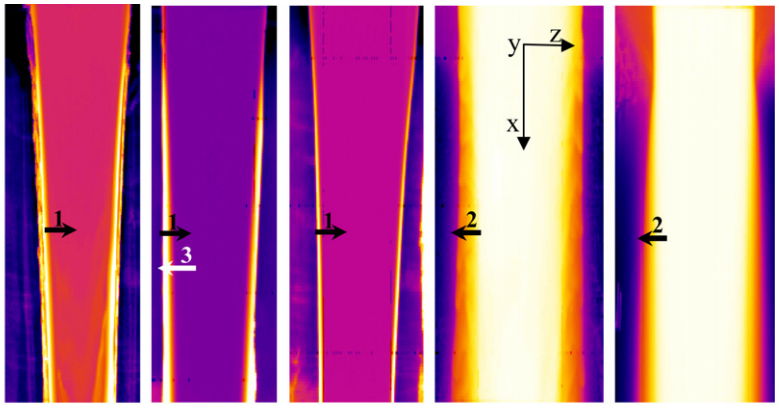

	Na_2SO_4	Ethanol	Glycerol	Ethanol	Glycerol
c	0.05	0.12	0.48	0.10	0.48
T_0 (°C)	30	25	25	50	50
T_h(°C)	70	70	70	0	0

Fig. 5. Thermal images of heated/cooled films at 0.36 kg m^{-1} s^{-1}. Black arrow: thermal Marangoni flow. White arrow: solutal Marangoni flow.

evaporation of ethanol. Fanton and Cazabat [22] have explored the spreading of liquid films driven by surface tension gradients induced by evaporation from a two-component mixture. As shown in the thermal image of heated ethanol–water film, the temperature of the film boundary is much higher than that of the film center, causing significant evaporation in the film boundary and thus the concentration gradient from the boundary to the center of the film. Since the surface tension of the ethanol aqueous solution increases with the decreasing concentration of ethanol, the concentration variations across the heated ethanol–water film finally induces the surface tension gradient from the center to the boundary of the film, causing the solutal Marangoni flow (shown as arrow 3) to weaken the gradient and eventually extends the film. In general, the thermal Marangoni flow in the lateral direction makes the heated film contracted and the cooled film extended. Here in the heated ethanol–water film, the solutal Marangoni effect probably overcomes the thermal Marangoni effect and extends the film. This is quite considerable since $|S_c|$ is much larger than $|S_T|$, as mentioned above. Practically, in the experiments, the periodical flow from the center to the boundary of the film could be clearly observed. However, since the glycerol–water mixture and aqueous Na_2SO_4 solution are of less volatility, the concentration of these two mixtures scarcely changed even after the experiments were run for several hours, and thus the solutal Marangoni effect can be ignored in the films of these solutions.

3.2.1. Shrinkage model for the heated films

By considering thermal Marangoni effect in the heated falling liquid film, we have derived a shrinkage model that can satisfactorily describe the Marangoni flow of heated water films [11]. In this model, the contracted width of the heated falling film on one side can be expressed as [11]:

$$\Delta Z = \frac{\sqrt{2}}{6}\frac{u}{K}\left[\left(S_x^{3/2} - S_0^{3/2}\right) - 3\left(S_x^{1/2} - S_0^{1/2}\right)\right] \tag{6}$$

where

$$x \in [0, x_e]$$

$$S_x = \left[\left(\frac{2H + 2Kx}{u}\right)^2 + 1\right]^{1/2} + 1$$

$$S_0 = \left[\left(\frac{2H}{u}\right)^2 + 1\right]^{1/2} + 1$$

$$\frac{H}{u} = \frac{\sigma_0}{\mu u}\cdot\frac{\delta}{4D}\left(1 - \frac{\sigma_w}{\sigma_0}\cos\theta\right)$$

$$\frac{K}{u} = \frac{3}{5D}\cdot\frac{\gamma(T_w - T_0)a}{\mu u^2\delta}$$

In Eq. (6), x_e represents the length of the contracted film. D stands for the width of the rim part. σ_0 and σ_w are surface tension at the temperature of T_0 and T_w, respectively. Moreover,

$$\delta = \left(\frac{3\mu\Gamma}{\rho^2 g}\right)^{1/3} \quad \text{and} \quad u = \frac{1}{2}\left(\frac{\rho g}{\mu}\right)\delta^2$$

In this work, the comparison of the shrinkage model with the experimental results was shown in Fig. 6. The symbols represent the experimental results while the single lines are results calculated from Eq. (6). Fig. 6 indicates that the model is in good agreement with the experimental data of the heated glycerol–water film. It should be noted that Eq. (6) is suitable for the case of liquid with less volatility, such as water, glycerol–water system, etc. As for the ethanol–water film, the theoretical model is hard to be derived since the temperature and concentration both vary and interact. Moreover, the study on theoretical model for the cooled film is currently on the way.

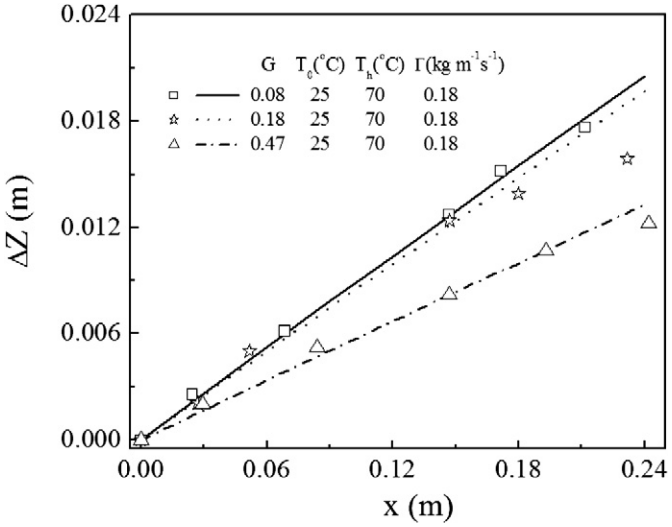

Fig. 6. Comparisons of the shrinkage model with experimental data.

3.2.2. Heated falling films

The heat transfer and flow characteristics of the heated films composed by a single component have been widely reported recently, covering the deformation of the film [8], different flow patterns [23], heat transfer to liquid rivulets or falling films [24,25], the thermocapillary instabilities [9] and contraction of heated water film [11,12]. This work was performed to examine the heat transfer and surface tension effect of binary liquid mixture films flowing over a heated plate.

With the help of the Thermal Imaging System, the wall temperature T_W and the film interfacial area A can be accurately obtained. This makes it convenient to calculate the heat transfer coefficient of the liquid film and the Nusselt number with the following equations:

$$\text{heat transfer coefficient}: \quad h = \frac{\rho C_P Q(T_{\text{out}} - T_0)}{A(T_W - T_f)} \tag{7}$$

$$\text{Nusselt number}: \quad Nu = \frac{h\cdot l_v}{\lambda} \tag{8}$$

where, Q is the volume flow rate and h represents heat transfer coefficient. $l_v = (\nu^2/g)^{1/3}$ stands for the viscosity length, in which ν denotes the kinematic viscosity and g the gravity acceleration. As shown in Fig. 7, the increase of Reynolds number results in the reinforced Nusselt number of the heated glycerol–water films, unlike the Kabov's conclusion that the heat transfer coefficient decreased with an increasing *Re* in the locally heated film [8]. This can be explained that Reynolds numbers in the present work are much higher than those in Kabov's work and

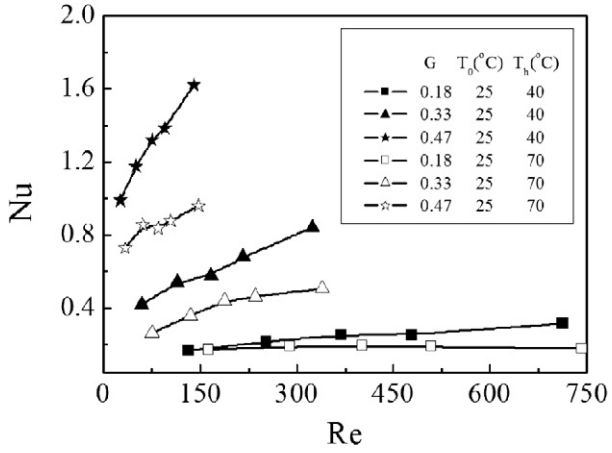

Fig. 7. Variations of *Nu* with *Re* for the glycerol–water films.

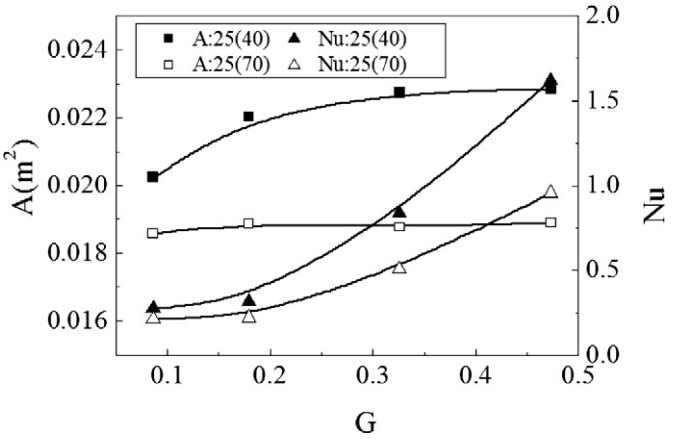

Fig. 8. The interfacial area and *Nu* of heated glycerol–water films at 0.36 kg m^{-1} s^{-1}. 25 (40) means $T_0 = 25\,^{\circ}\mathrm{C}$, $T_h = 40\,^{\circ}\mathrm{C}$.

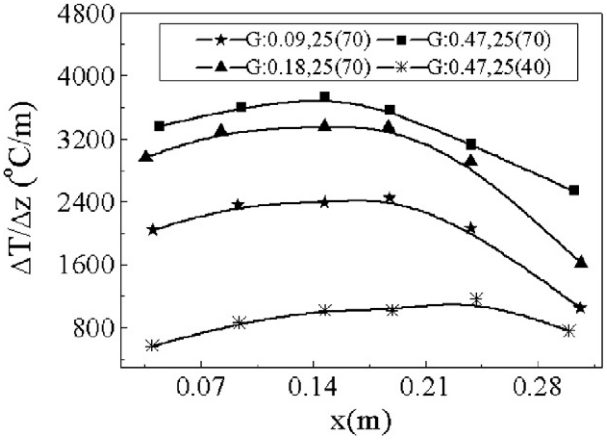

Fig. 9. Lateral surface temperature gradient in the heated glycerol–water films. 25 (70) means $T_0 = 25\,^{\circ}\mathrm{C}$, $T_h = 70\,^{\circ}\mathrm{C}$. G: 0.09 means that the weight fraction of glycerol is 0.09.

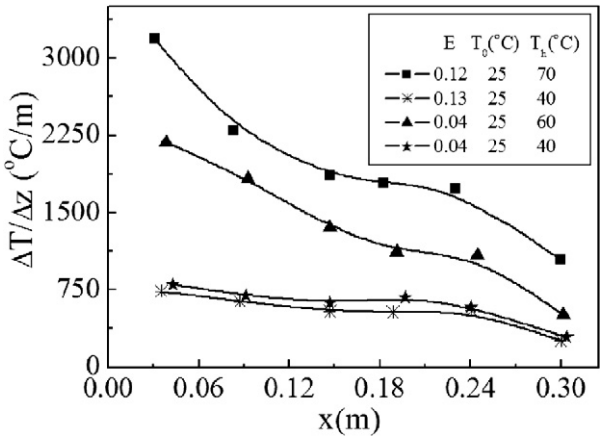

Fig. 10. Variations of $\Delta T/\Delta z$ with x in the heated ethanol–water film.

our films are heated uniformly, therefore the particular thermocapillary structure observed by Kabov does not occur in our experiments.

As can be seen in Fig. 8, for the same T_0, the interfacial area A at $T_h = 40\,^{\circ}\mathrm{C}$ is larger than that at $T_h = 70\,^{\circ}\mathrm{C}$, since there is more effective Marangoni forces to contract the film, causing a smaller A when $T_h = 70\,^{\circ}\mathrm{C}$. As shown in Fig. 9, for the heated glycerol–water films, the higher concentration of glycerol induced greater lateral surface tension gradient (thermal Marangoni flow) which is to contract the film more distinctly. However, since the increase in concentration of glycerol also induces the larger viscosity which generally weakens the liquid flow, the contraction of the film is limited and the interfacial area stands larger for heated glycerol–water film of higher concentration (see Fig. 8).

The lateral surface temperature gradient in the heated glycerol–water films is illustrated in Fig. 9, showing that for the heated glycerol–water film, the averaged temperature gradient $\Delta T/\Delta z$ increases with a rise in G, and the higher heating temperature leads to the larger value of $\Delta T/\Delta z$ at a given G. Furthermore, $\Delta T/\Delta z$ rises gradually with an increase of x when x is less than a certain value (i.e. 0.17), then it sharply drops when x further increases.

Different from the cases of glycerol–water films, as shown in Fig. 10, $\Delta T/\Delta z$ decreases monotonously as the heated ethanol–water films flowing downwards. On the other hand, in the heated ethanol–water film, the higher heating temperature leads to the larger value of $\Delta T/\Delta z$. This is similar to the case of glycerol–water films. Notably, the variation of $\Delta T/\Delta z$ with x is more moderate under the lower T_h.

Due to the volatility of ethanol and the higher temperature in the boundary, there is considerable concentration gradient in the lateral direction of the heated ethanol–water films. This concentration gradient, as mentioned above, induces surface tension gradient from the film center to the boundary. It is shown in Fig. 11 that $\Delta\sigma_c/\Delta z$, the average surface tension gradient resulted from the concentration variations is negative as it is in the opposite direction of $\Delta\sigma_T/\Delta z$ (the averaged surface tension gradient arising from the temperature variations). Most significantly, the absolute value of $\Delta\sigma_c/\Delta z$ is at least 14 times larger than $\Delta\sigma_T/\Delta z$, thus the heated ethanol–water film is easily extended by solutal Marangoni effect.

Comparing to ethanol–water system, the concentration variations in glycerol–water system and Na_2SO_4–water system are unapparent, it is considerable to compare the thermal Marangoni effect between the working fluids. In general, the

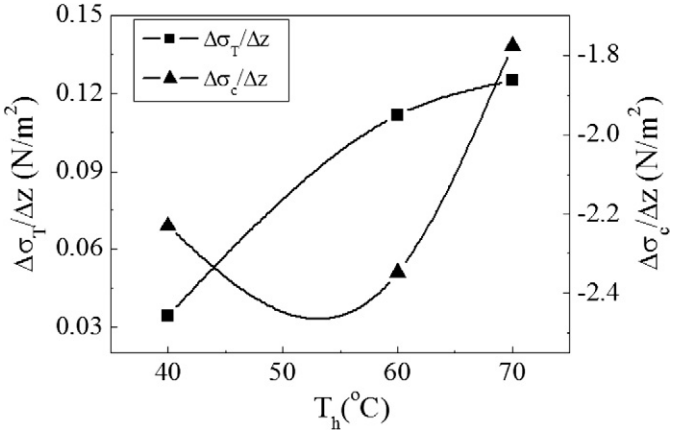

Fig. 11. Surface tension gradient based on the temperature variation and the concentration variation in the heated ethanol–water films.

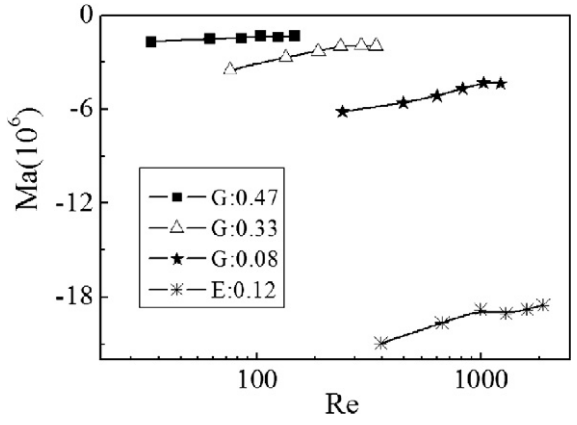

Fig. 12. Variations of *Ma* with *Re* at $T_0 = 25\,^{\circ}\mathrm{C}$, $T_h = 70\,^{\circ}\mathrm{C}$. *G*: 0.47 means that the weight fraction of glycerol is 0.47. *E*: 0.12 means that the weight fraction of ethanol is 0.12.

Marangoni effect induced by the temperature variations can be characterized by the Marangoni number:

$$Ma = \frac{\frac{\mathrm{d}\sigma}{\mathrm{d}T}(T_w - T_f)\cdot L}{\mu a} \tag{9}$$

where, L denotes the heater's length and $a = \lambda/\rho C_p$ the heat diffusivity of the liquid. Eq. (9) indicates that the thermal Marangoni effect is generally reinforced by the large heating temperature difference and is weakened by the strong viscosity. As displayed in Fig. 12, *Ma* is negative for the heated films, since $\mathrm{d}\sigma/\mathrm{d}T$ is negative for the liquids used in the present work. It can be seen that increasing *Re* causes a slight rise in *Ma*. For the glycerol–water film, *Ma* increases with the rising *G* (due to the greater viscosity), well agreed with Cazabat's conclusion [3]. This is also consistent with the changes of S_T versus T as displayed in Fig. 2. Likewise, due to the less viscosity, $|Ma|$ in the heated ethanol–water films is significantly larger than that in the glycerol–water films.

Table 2 shows the influence of Na_2SO_4 concentration on the interfacial area, Nusselt number and Marangoni number at 0.36 kg m^{-1} s^{-1}. It is found that when $C_{Na_2SO_4} = 0.05$, the interfacial area and Marangoni number reach the maximum whereas *Nu* number is the smallest. Moreover, the interfacial area and the absolute Marangoni number of aqueous Na_2SO_4 film is close to those of the glycerol–water film, but less than that of the ethanol–water film.

Table 2
The interfacial area, *Nu* and *Ma* of Na_2SO_4 aqueous film at 0.36 kg m^{-1} s^{-1}

$C_{Na_2SO_4}$	A (m^2)	*Nu*	*Ma* (10^6)
0.00	0.0167	0.214	−3.89
0.01	0.0179	0.154	−4.97
0.05	0.0185	0.150	−5.20
0.10	0.0180	0.173	−4.37

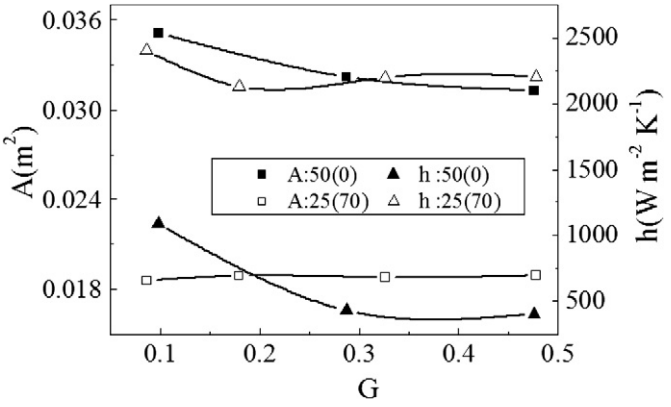

Fig. 13. Comparisons of interfacial area and heat transfer coefficient between the heated and cooled films.

3.2.3. The cooled films

The heated films were widely studied with experimental and theoretical methods for industrial purposes. However, for the cooled films, few investigations have been reported even though the cooling film operations are also very important in the transfer processes. In the present work, binary mixture films flowing down a plate at a temperature lower than the film temperature were investigated.

It can be found in Fig. 5, that the cooled films are gradually expanded. This means that the interfacial area of the cooled film is eventually enlarged (comparing to the interfacial area of the isothermal liquid films). The comparisons of the interfacial area and heat transfer coefficient for heated and cooled films are given Fig. 13, showing that the cooled films have larger interfacial area *A* than the heated films, while the heat transfer of the heated films is stronger due to the small viscosity of the liquid in the heated film's substrate. Practically, the film substrate controls the heat transfer of the film, i.e., the heat transfer is enhanced when the film substrate becomes thinner. Notably, *A* drops with the increasing *G* for the cooled films, but increases with the rise of *G* for the heated films.

Nu and *A* of the glycerol–water films are displayed in Fig. 14, showing that the lower T_h enhances Nusselt number and enlarges *A* for the cooled films. Meanwhile, *Nu* increases and *A* decreases with the increasing glycerol concentration, due to the significant high viscosity.

The variations of the average temperature gradient over the film width versus x in the cooled ethanol–water films, as illustrated in Fig. 15, indicate that the average temperature gradient,

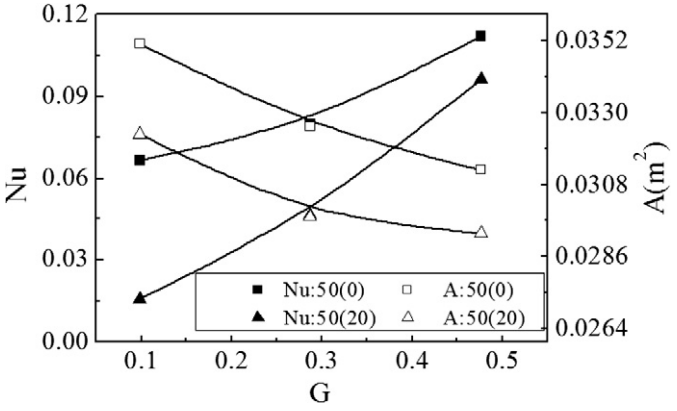

Fig. 14. The interfacial area and *Nu* of cooled glycerol–water films at 0.36 kg m^{-1} s^{-1}.

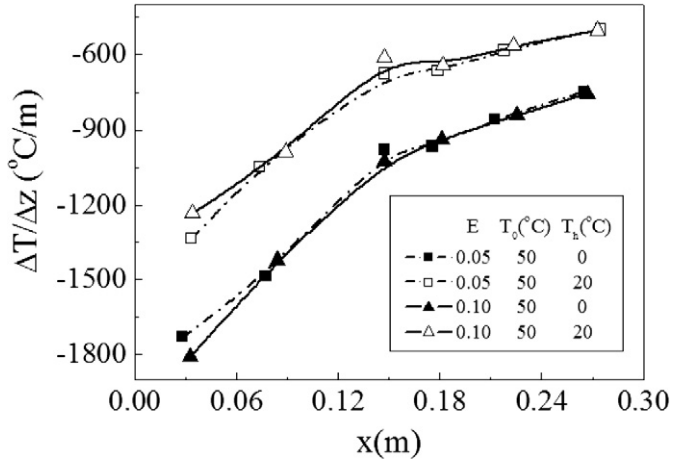

Fig. 15. Lateral surface temperature gradient in the cooled ethanol–water films.

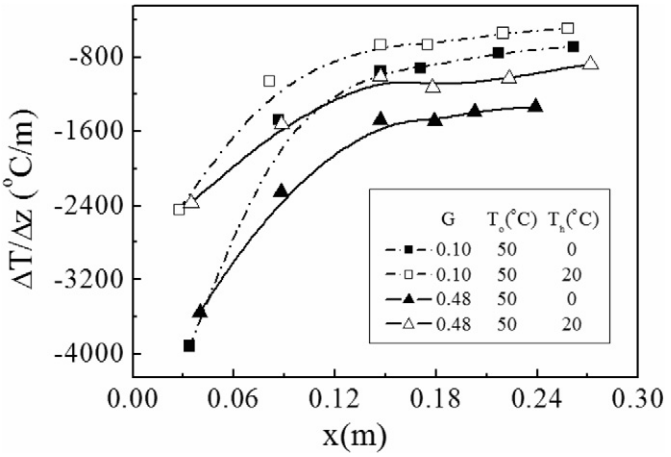

Fig. 16. Lateral surface temperature gradient in the cooled glycerol–water films.

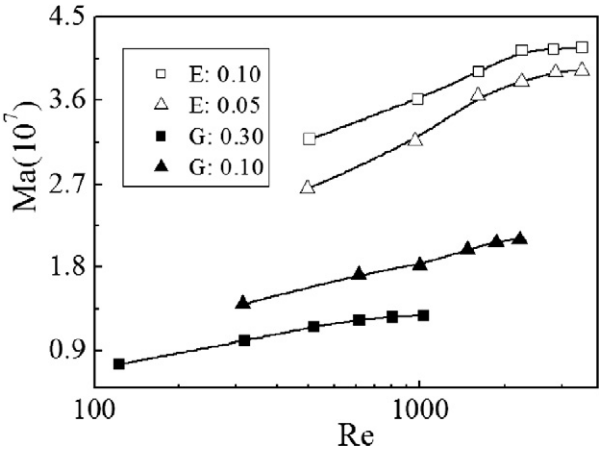

Fig. 17. Variations of *Ma* with *Re* at $T_0 = 50\,^{\circ}\mathrm{C}$, $T_h = 0\,^{\circ}\mathrm{C}$.

$\Delta T/\Delta Z$ is negative and rises with the increasing x. Obviously, a critical value x_c (about 0.15 m) exists in each curve of $\Delta T/\Delta Z$ versus x, i.e., when x is less than x_c, $\Delta T/\Delta Z$ rises sharply with the increasing x, and when $x > x_c$, the increment is weakened. It can be further found in Fig. 15 that $\Delta T/\Delta Z$ is scarcely changed with the ethanol concentration, but keeps sensitive to the heating temperature difference. The higher value of $T_0 - T_h$ leads to the larger value of $|\Delta T/\Delta Z|$ at the same ethanol concentration. The comparison of Fig. 15 with Fig. 10 indicates that the variations of $|\Delta T/\Delta Z|$ with x are quite similar for the both cases of heated and cooled ethanol–water films. As for the cooled glycerol–water films, Fig. 16 shows that there are also such critical values of x existing in the curves of $\Delta T/\Delta Z$ versus x. At the same G, the lower value of $T_0 - T_h$ results in the higher $\Delta T/\Delta Z$. Moreover, $|\Delta T/\Delta Z|$ increases with a rise in glycerol concentration, since the larger viscosity retards the liquid flow and thus weakens the heat transfer.

According to Eq. (9), the thermal Marangoni number for a cooled film is positive, due to $T_w - T_f > 0$. Fig. 17 gives the plots of the Marangoni number versus *Re*. As can be seen, increasing *Re* results in enhanced *Ma*. Meanwhile, the higher concentration leads to the larger *Ma* for the ethanol–water films. This is quite consistent with the variations of $|S_T|$ versus the concentrations of ethanol as shown in Fig. 2.

4. Conclusions

The flow characteristics and heat transfer of heated/cooled liquid films of water, ethanol aqueous solutions, glycerol aqueous solutions and aqueous Na_2SO_4 solutions, were investigated with a thermal imaging technique under the wide range of flow rate, concentration and heating temperature difference.

Distinct surface temperature gradient exists in the heated/cooled films, causing the contraction/extension of heated/cooled films of glycerol aqueous solutions and aqueous Na_2SO_4 solutions. For the heated ethanol–water film, the solutal Marangoni effect, due to the efficient evaporation of ethanol in the film rim, overcomes the thermal Marangoni effect and causes the extension of the film. The experiments show that the surface tension gradient caused by the concentration variations is at least 14 times larger than that induced by temperature gradient. Theoretical analyses also reveal that $|S_c|$ of the working liquids used in the present work is significantly higher than $|S_T|$. $|S_c|$ of ethanol–water solution is larger than $|S_c|$ of glycerol–water solution, indicating that more significant surface tension effect can be caused by the ethanol concentration variations. The viscosity has complex influence on the interfacial area, heat transfer and temperature gradient of the heated/cooled liquid films. Larger viscosity gener-

ally induces greater temperature gradient and thus larger surface tension gradient (Marangoni flow), but retards the liquid flow.

Acknowledgements

The authors are grateful to the financial support from the National Natural Science Foundation of China (No. 20576050).

References

[1] C.V. Sternling, L.E. Scriven, Interfacial turbulence: hydrodynamic instability and the Marangoni effect, AIChE J. 5 (1959) 514–523.
[2] L.E. Scriven, C.V. Sternling, The Marangoni effects, Nature 167 (1960) 186–188.
[3] A.M. Cazabat, F. Heslot, S.M. Troian, P. Carles, Fingering instability of thin spreading films driven by temperature gradients, Nature 346 (1990) 824–826.
[4] A. D'Aubeterre, R.D. Silve, M.E. Aguilera, Experimental study on Marangoni effect induced by heat and mass transfer, Int. Com. Heat Mass Trans. 32 (2005) 677–684.
[5] D. Sultanovic, et al., A study of the heat transfer of rivulet flow on inclined plates, Solar Energy 60 (1997) 221–227.
[6] E. Sultan, A. Boudaoud, M.A. Ben, Evaporation of a thin film: diffusion of the vapour and Marangoni instabilities, J. Fluid Mech. 543 (2005) 183–202.
[7] A.E. Hosoi, J.W.M. Bush, Evaporative instabilities in climbing films, J. Fluid Mech. 442 (2001) 217–239.
[8] O.A. Kabov, B. Scheid, I.A. Sharina, J.C. Legros, Heat transfer and rivulet structures formation in a falling thin liquid film locally heated, Int. Therm. Sci. 41 (2002) 664–672.
[9] S.W. Joo, S.H. Davis, S.G. Bankoff, A mechanism for rivulet formation in heated falling films, J. Fluid Mech. 321 (1996) 279–298.
[10] S.W. Joo, S.H. Davis, S.G. Bankoff, Long-wave instability of heated falling films: two-dimensional theory of uniform layers, J. Fluid Mech. 230 (1991) 117–146.
[11] F. Zhang, Z.B. Zhang, J. Geng, Study of contraction characteristics of heated falling liquid films, AIChE J. 51 (2005) 2899–2907.
[12] F. Zhang, J. Geng, S.L. Ma, Z.B. Zhang, The influence of Marangoni effect on heated falling films, J. Chem. Ind. Eng. (China) 56 (2005) 1606–1611.
[13] P. Ehrhard, S.H. Davis, Non-isothermal spreading of liquid drops on horizontal plates, J. Fluid Mech. 229 (1991) 365–388.
[14] F. Ziegler, G. Grossman, Heat-transfer enhancement by additives, Int. J. Refrig. 19 (1996) 301–309.
[15] W.L. Cheng, K. Houda, Z.S. Chen, A. Akisawa, P. Hu, T. Kashiwagi, Heat transfer enhancement by additive in vertical falling film absorption of H_2O/LiBr, Appl. Therm. Eng. 24 (2004) 281–298.
[16] J. Castro, L. Leal, C.D. Pérez-Segarra, P. Pozo, Numerical study of the enhancement produced in absorption processes using surfactants, Int. J. Heat Mass Trans. 47 (2004) 3463–3476.
[17] Z.F. Sun, K.T. Yu, Rayleigh–Benard–Marangoni cellular convection—Expressions for heat and mass transfer rates, Chem. Eng. Res. Des. 84 (2006) 185–191.
[18] Y. Utaka, S. Wang, Characteristic curves and the promotion effect of ethanol addition on steam condensation heat transfer, Int. J. Heat Mass Trans. 47 (2004) 4507–4516.
[19] C. Philpott, J. Deans, The enhancement of steam condensation heat transfer in a horizontal shell and tube condenser by addition of ammonia, Int. J. Heat Mass Trans. 47 (2004) 3683–3693.
[20] A.E. Hosoi, J.W.M. Bush, Evaporative instabilities in climbing films, J. Fluid Mech. 442 (2001) 217–239.
[21] A.L. Horvath, Handbook of Aqueous Electrolyte Solutions: Physical Properties, Estimation and Correlation Methods, Ellis Horwood, West Sussex, 1985.
[22] X. Fanton, A.M. Cazabat, Spreading and instabilities induced by a solutal Marangoni effect, Langmuir 14 (1998) 2554–2561.
[23] O.A. Kabov, E.A. Chinnov, Heat transfer from a local heat source to a subcooled falling liquid film, Russ. J. Eng. Thermophys. 7 (1997) 1–34.
[24] A.B. Ponter, G.D. Davis, Heat transfer to falling films, Chem. Eng. Sci. 23 (1968) 664–665.
[25] D. Sultanovic, B. Bjerke, J. Rekstad, et al., A study of the heat transfer of rivulet flow on inclined plates, Solar Energy 60 (1997) 221–227.